Topography of contextual modulations mediated by short-range interactions in primary visual cortex

Aniruddha Das & Charles D. Gilbert

The Rockefeller University, 1230 York Avenue, New York, New York 10021, USA

Neurons in primary visual cortex (V1) respond differently to a simple visual element presented in isolation from when it is embedded within a complex image. This difference, a specific modulation by surrounding elements in the image, is mediated by short- and long-range connections within V1 and by feedback from other areas. Here we study the role of short-range connections in this process, and relate it to the layout of local inhomogeneities in the cortical maps of orientation and space. By measuring correlation between neuron pairs located in optically imaged maps of V1 orientation columns we show that the strength of local connections between cells is a graded function of lateral separation across cortex, largely radially symmetrical and relatively independent of orientation preferences. We then show the contextual influence of flanking visual elements on neuronal responses varies systematically with a neuron's position within the cortical orientation map. The strength of this contextual influence on a neuron can be predicted from a model of local connections based on simple overlap with particular features of the orientation map. This indicates that local intracortical circuitry could endow neurons with a graded specialization for processing angular visual features such as corners and T junctions, and this specialization could have its own functional cortical map, linked with the orientation map.

The response of a neuron in primary visual cortex (V1) to an element of a complex image is influenced significantly by the context surrounding that element[1]. The specific layout of the surrounding features can facilitate or suppress the neuronal response and alter its temporal structure markedly, compared to the response to the same element presented in isolation. It is assumed that this modulation is involved in the analysis of form. Investigation of the physiological substrates of these context-dependent interactions has focused largely on long-range horizontal connections in V1[2–4] that are believed to be involved in perceptual grouping and contour saliency[5–7]. Less attention has been paid to the role of local connections between neighbouring cells.

The effective local intracortical connections of a neuron—and the consequent local visual processing—are likely to depend strongly on the location of the neuron in the cortical maps of orientation and space. Maps of orientation columns over the surface of VI show varying degrees of local homogeneity. Cortical columns where orientation preference changes smoothly or remains essentially constant over distances of 500 μm or more are interspersed with regions containing orientation singularities—reversals, sharp jumps (fractures) and point singularities[8–11] where the orientation changes by up to 90° in less than 150 μm. The map of retinotopy on VI may show similar inhomogeneities that correlate closely with inhomogeneities in the map of orientation[12]. Neurons within a cortical column of uniform orientation have largely overlapping receptive fields, whereas neurons separated by as little as 150 μm across an orientation fracture (which have mutually orthogonal orientation preferences) have largely non-overlapping receptive fields. However, anatomical studies indicate that the dendritic and local axonal arborizations of pyramidal neurons are largely circularly symmetrical, and extend laterally out by 300–500 μm independently of the neuron's proximity to functional boundaries such as orientation singularities[13] or other functional features within V1 (refs 14–16). Neurons close to orientation singularities are thus likely to be anatomically connected to neurons preferring a range of orientations, including orthogonal ones, in neighbouring cortical columns[17]. By contrast, neurons distant from orientation singularities, lying within a region of uniform orientation, are linked anatomically with a more homogeneous population of cells having similar orientation preferences and receptive fields.

Here we explore whether these patterns of local anatomical connectivity translate to similar patterns of effective physiological connection strength, and the role that such local connections have in the visual processing of complex images. We address two questions: first, how much does the effectiveness of local physiological connections depend on cortical distance, compared to the relative preferred orientations of two cells? Second, does the pattern of local connections predict the nature of neuronal responses to complex visual stimuli, and, in particular, the influence of local visual context on a neuron's response to its preferred stimuli? For this second question we restricted our study to visual contexts provided by line elements orthogonal to the preferred orientation of the recorded neuron[18–20], to probe selectively the local—as opposed to long-range—cortical connectivity. The modulation of a neuron's activity by iso-oriented flanking stimuli is believed to involve long-range horizontal connections that selectively interconnect cortical columns of similar orientation preference in V1 (refs 21–24). The influence of perpendicular flanking bars is thus likely to be the least dependent on long-range circuitry[17]. All experiments were done in cat V1 using optical imaging of intrinsic signals (that is, changes in cortical reflectance linked to metabolic changes resulting from local neural activity[25,26]) and electrophysiological recordings from neurons in upper layers (up to 400 μm deep).

Distribution of local connection strengths

We measured the strengths of connections between pairs of neurons as a function of cortical separation and relative orientation difference, using the measure of cross-correlation strength. Earlier experimental results and theoretical considerations indicate that the height and area of the correlation peak for a pair of neurons,

normalized by the correlation baseline, gives an estimate of the 'effective connection strength' between the neurons[23,27–32]. Recording sites were chosen after obtaining an optical map of V1 orientation columns and the recorded neurons were driven with optimally oriented line stimuli.

Using cross-correlation, we found strong effective physiological connections between pairs of neurons of all relative orientation preferences and at lateral separations of up to about 800 μm. This was true even for pairs of neurons that had mutually orthogonal preferred orientations (Fig. 1a), with sharp orientation tuning, non-overlapping receptive fields and no common responses to single bars at any orientation (Fig. 1a). When we held one electrode fixed and moved the other to different sites, at roughly the same distance but with very different preferred orientations, we found correlation peaks that were similar in height and area (Fig. 1b), indicating that the effective physiological connection strengths between pairs of neurons at comparable lateral separations is largely independent of orientation preferences.

We controlled for the null hypothesis that only neuron pairs with similar orientation preferences are significantly cross-correlated and that the correlation obtained for orthogonally oriented neurons was an artefact of inadequate spike isolation. Such an artefact could arise, when recording from orthogonal orientation columns, through contamination by a small fraction of spikes from cells having the same, rather than the orthogonal, orientation preference. This fraction could be small enough that orientation tunings for the two sites appear orthogonal, but the contaminating subset of spikes could be the ones actually generating a significant cross-correlogram and be responsible for the apparently strong correlations between orthogonally oriented neurons. Figure 1c shows the results of a control experiment to test for this possibility, with a pair of sites at a separation of 280 μm and relative orientation difference of 80°. One of the recording sites (red) was close to an orientation singularity, where the chance of contamination from units of different orientation preferences is high. If the correlogram obtained by optimally stimulating both of the nominally orthogonal channels (Fig. 1c, upper correlogram, not normalized by the baseline) were due to such contamination, then stimulating the

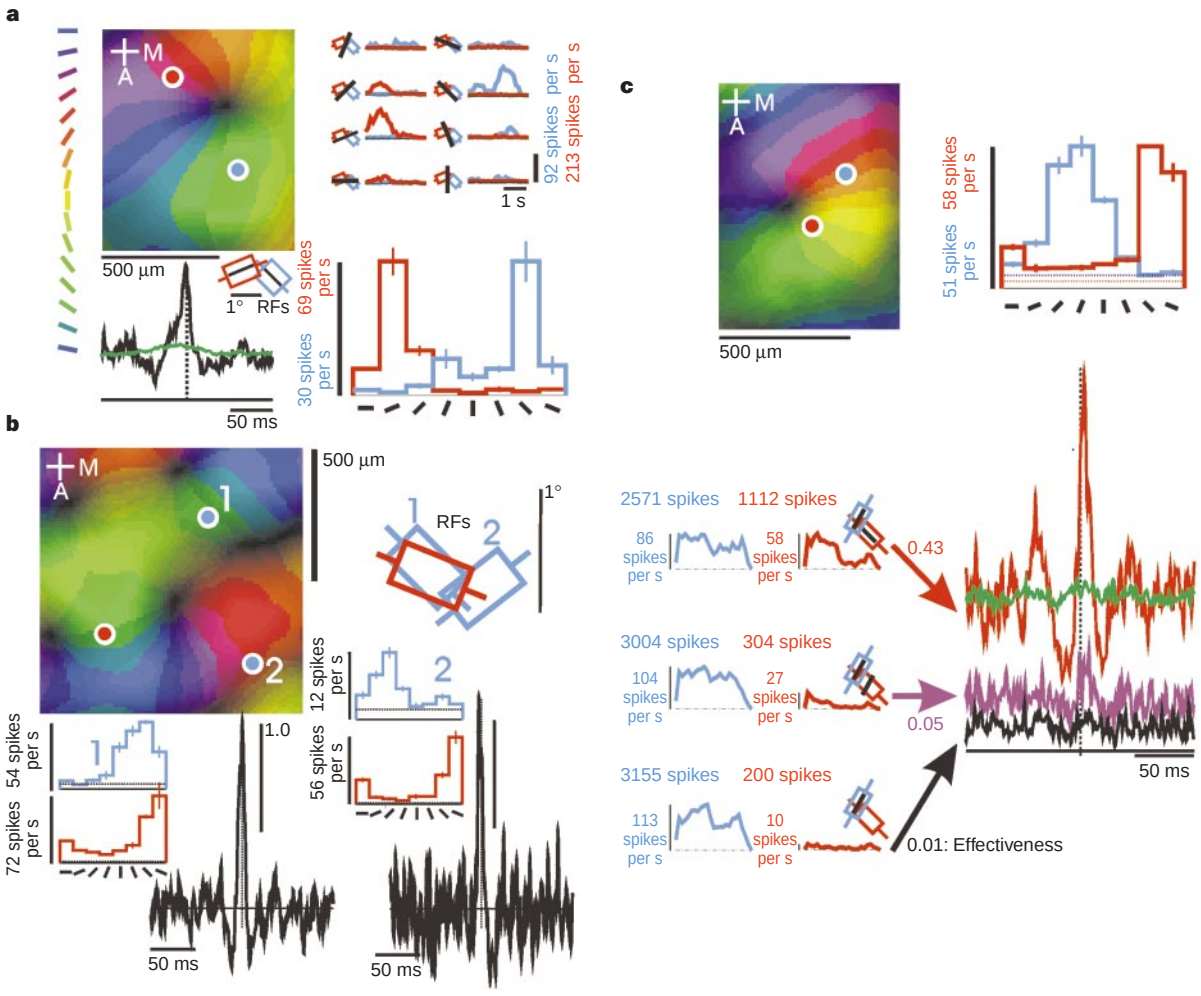

Figure 1 V1 neurons have strong local interconnections, independent of relative orientation difference. **a**, Results for a neuron pair with a 70° orientation-preference difference. Top left: optical image of orientation map with electrode recording sites. The corresponding receptive field (RF) outlines, PSTHs to single oriented bars (upper right) and orientation tuning curves (lower right) are colour-coded by recording site (blue and red). An independent colour code is used for the optical map (key to left of optical image, see Methods; black line to left of each PSTH, or below orientation tuning curve, indicates stimulus orientation). Lower left: cross-correlogram obtained with two-bar stimulus optimally driving both neurons simultaneously (black: raw correlogram; green: shuffled correlogram baseline; normalized peak height, 1.46). **b**, Comparing correlograms for neuron pairs with one common reference (the 'red' site). The 'blue' electrode was positioned in a similarly or orthogonally oriented column (sites 1 and 2, respectively). The corresponding receptive fields, orientation tuning curves and normalized, shuffle-corrected cross-correlograms are shown. **c**, Top: PSTHs and raw cross-correlogram (green: shuffled baseline) obtained by stimulating both 'red' and 'blue' receptive fields with optimally positioned and oriented bars. Middle: the same, but with stimulus bars that were both oriented for the 'blue' site. Bottom: the same, but using a single stimulus bar optimal for the receptive field 'blue' alone. The 'effectiveness[28]' (total number of spikes in raw peak/number of spikes in 'blue' channel) is shown for each case.

two channels by stimuli oriented for the reference channel (middle correlogram) or stimulating the reference receptive field alone (lower correlogram) should have preferentially driven the 'contaminating' spikes. We would then expect raw correlogram peaks of similar sizes. This was not the case, indicating that the cross-correlations between orthogonally oriented neurons are not due to such contamination. Note that the average spike rate and total number of spikes in the reference channel remained essentially the same for all three configurations of stimuli.

Our pooled results (from 85 neuron pairs) indicate that neighbouring upper-layer neurons in V1 have strong physiological connections with each other, largely independent of relative orien-

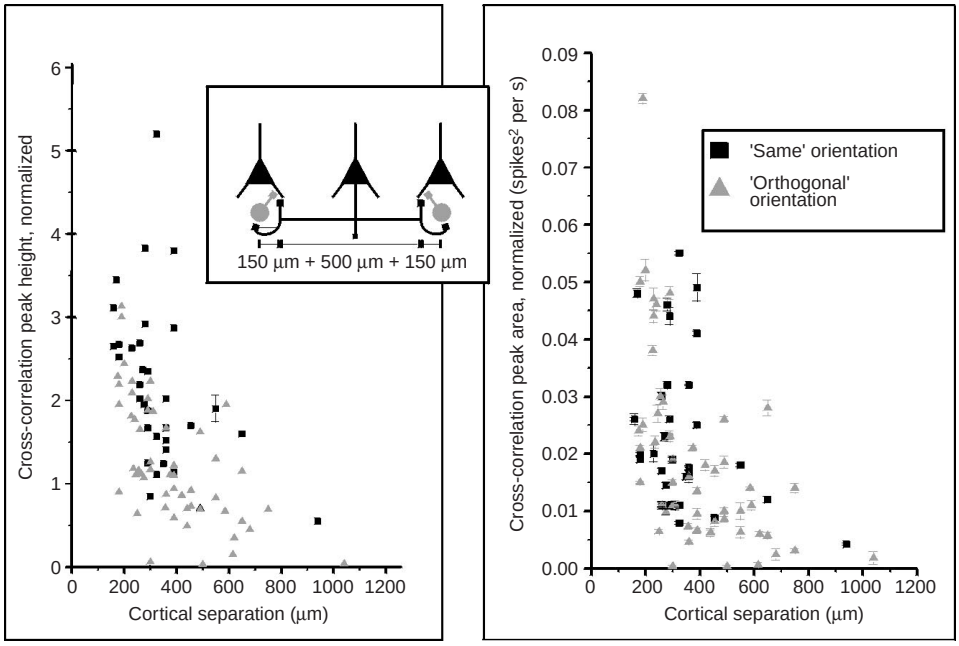

Figure 2 Normalized cross-correlation peak height (left) and peak area (right) for receptive field pairs as a function of inter-site separation on cortex. The full population is divided into 'similarly oriented' or 'orthogonally oriented' pairs. (Error bars, ±s.d. Only one (average) error bar is shown for peaks, to avoid clutter.) Inset: a plausible circuit of local interconnection between neurons separated by up to 800 μm: a source of common input with axonal arborization extending out to 500 μm in diameter could be connected to target neurons each with a dendritic arborization of 150 μm radius, both directly (excitatory connection) and through an inhibitory interneuron.

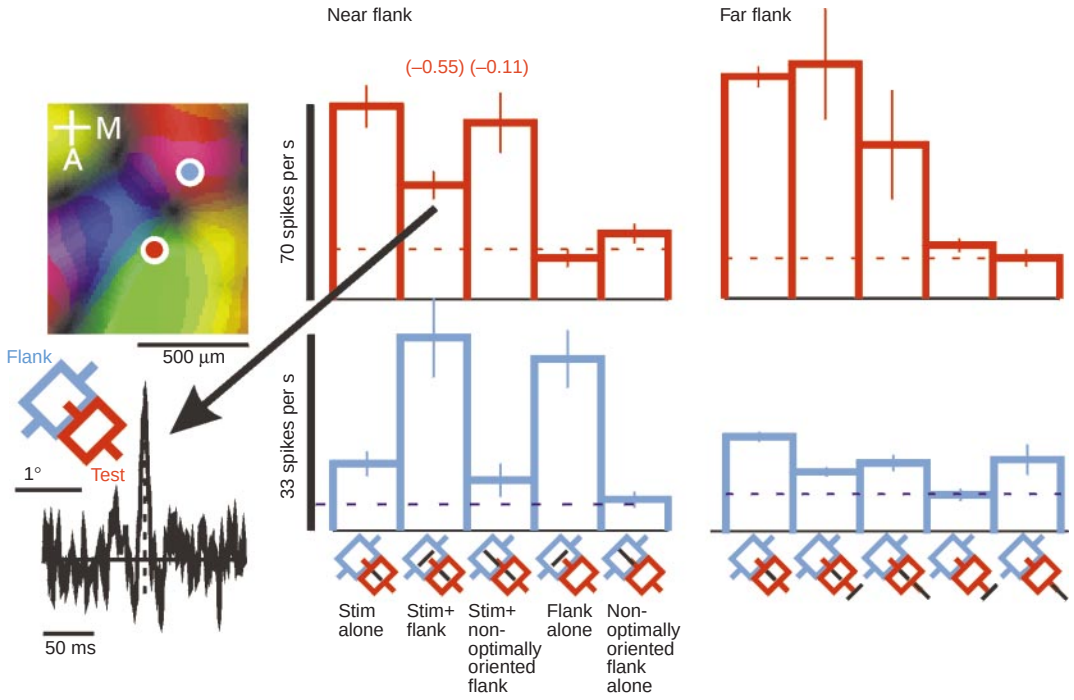

Figure 3 Specific suppressive influence of perpendicular flank stimuli. Top left: The test site (135° orientation) is labelled red; blue marks a recording site monitoring activation of the neighbouring cortical region of 45° orientation, selected as the flank. Right: Histograms of responses in the test and flank neurons. Black lines in the key below the flank response histogram indicate the stimulus configuration for each pair of test and flank responses; numbers in parenthesis quantify test suppression (see Methods; error bar, ± s.e.m.; $n = 11$). Lower left: Cross-correlogram obtained from the spike trains stimulated by the 'Near flank', 'Stim + flank' configuration. (Correlogram shuffle-corrected and normalized: peak, 0.79; area, 0.006.)

tation preferences. The connection strength is a graded function of cortical distance, at a spatial scale consistent with anatomical connectivity. For relatively short cell separations of up to about 800 μm, the cross-correlation peak sizes, and particularly peak areas, were independent of relative orientation difference over the population (Fig. 2) and were essentially a function of inter-site separation. All the cross-correlation peaks measured had a significant value at $\tau = 0$, implying that a large portion of the synaptic input captured by the correlation process is of the common input type. A lateral separation of 800 μm, though large, is consistent with the known anatomy of local axonal connections. Pyramidal neurons in upper layers of cat V1 have local axonal arborizations up to 500 μm in diameter and dendritic arborizations up to 300 μm in diameter. Thus pyramidal neurons can provide a common input to upper layer neurons separated by up to 800 μm (inset, Fig. 2). Note that the connections providing common inputs are likely to be directly excitatory as well as having an inhibitory component through local inhibitory interneurons[33–35] (inset, Fig. 2). The range of correlation peak heights for 'same orientation' neuron pairs appeared to be slightly higher than the range for 'orthogonal' neuron pairs, presumably reflecting narrower correlogram peaks (Fig. 2), that is, a tighter temporal correlation. The effective connection strengths between neuron pairs are, however, more reliably related to normalized correlogram peak areas, which showed little such bias overall in the population, rather than to peak heights[27,31].

Local circuitry and contextual modulation

The above analysis implies that the local circuits for visual processing in V1 include strong lateral connections with nearby orientation columns. Over a spatial scale of 500–800 μm, these connections are largely independent of the orientation preferences of the columns. Owing to inhomogeneities in the maps of orientation and space, which repeat at roughly the same scale of 500–800 μm, the relative orientations and receptive field positions of neurons that make up a local neighbourhood vary considerably with their positions on the cortex. We investigated the consequences, for neuronal processing of complex stimuli, of this pattern of local connectivity and its systematic variation across the cortex. As a probe of contextual modulation we used flanking perpendicular lines, lying immediately outside the classical receptive field, which influence the responses of neurons to optimal stimuli within their receptive fields. After obtaining the optical map of orientation columns we chose a 'test' recording site lying in a cortical column of a given orientation preference. This site was situated at a specific distance from a neighbouring cortical region of orthogonal orientation preference (the chosen 'flank' cortical region to be driven by flanking perpendicular stimuli). Using electrode recordings, we mapped the distribution of receptive fields represented in the local area of cortex. Short line segments of optimal size, orientation and position were then used to drive, selectively, neurons in the recording site and in the flanking region of cortex.

The primary influence of flanking perpendicular visual stimuli was to suppress the responses of neurons to their optimal stimuli, particularly when the contrast of the flank stimulus bar was more than twice that of the bar within the receptive field (Fig. 3). After optically imaging the orientation map, we positioned two electrodes in two neighbouring, orthogonally oriented cortical columns. One of the recording sites was then selected as the test site and its corresponding optimal stimulus as the test stimulus. The other neuron's receptive field ('flank receptive field') was used to position the flank stimulus (Fig. 3). The flank neuron's responses were monitored as a measure of the activity of neurons in the corresponding cortical region (the flank cortical region for this particular configuration) for different combinations of test and flank stimuli. A bar stimulus optimally oriented and positioned to drive the flank neuron led to a 55% reduction in the response of the test neuron to its own optimal stimulus (Fig. 3, 'Stim + flank'). Only stimuli that specifically drove the neighbouring flanking region of cortex led to such a reduction in the signal strength in the test neuron. A bar at the same position in visual space, inside the flank receptive field but no longer optimally oriented to drive flank neurons (Fig. 3,

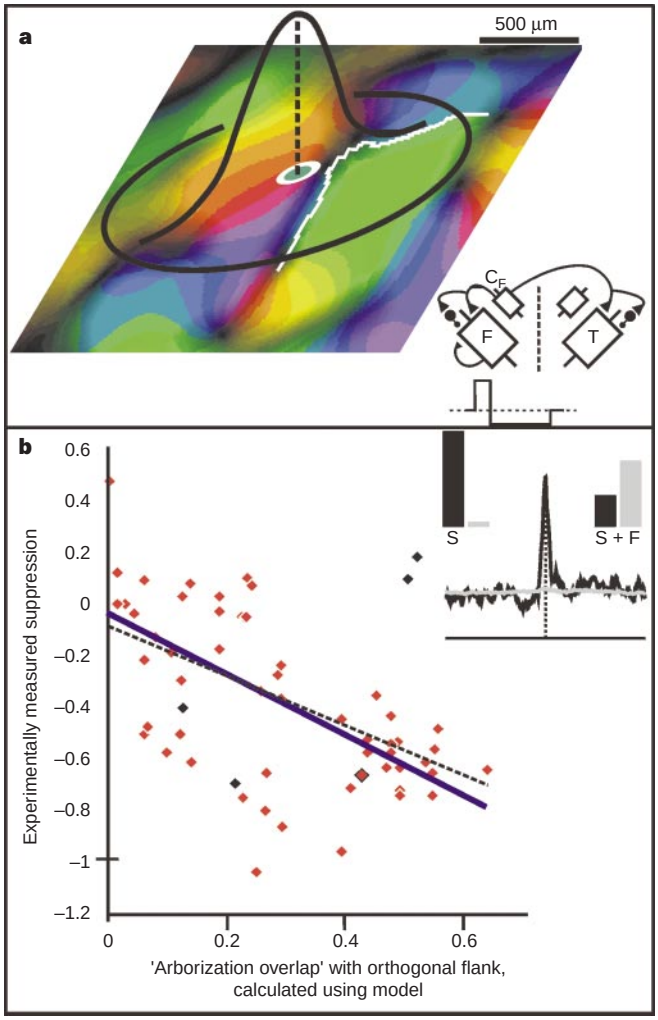

Figure 4 Comparing suppression strength with arborization overlap calculated using geometric model. **a**, Quantitative model of arborization overlap (see Methods) illustrated for a specific recording site within a 45° cortical column but close to a 135° column. The white outline marks the flank cortical region selected by the model as 'orthogonal' in orientation to the recording site. Inset: model to simulate suppression by flank stimuli, mediated through common input (Fig. 3; see Methods). T and F represent simultaneously recorded test and flank neurons, in orthogonal cortical columns separated by a singularity (dashed line). C_F represents other neurons in the flank column, providing direct excitatory input (triangles) and di-synaptic inhibitory input (circles) to both F and T. Units in the test column provide similar, mirror-image connections (not shown). The profile of each common-input excitatory, followed by inhibitory, modulation is indicated below the circuit. **b**, Experimentally measured suppression plotted as a function of the corresponding model, arborization overlap. (The four points in black mark the far/near pairs where 'near' suppression was weaker than 'far', Fig. 5c. Blue line: regression fit, $n = 56$, $R^2 = 0.39$, through all points excluding the four in black; black dotted line: $n = 60$, $R^2 = 0.25$, through all points.) Inset: results of simulated suppression by flank. S: simulated response histograms when only test column was activated; S + F: with simulated activity in flank neuron, the test response is suppressed. The normalized cross-correlogram of the test and flank spike trains simulated in the S + F condition is also shown. (Simulated test response histogram shown in black, flank in grey). See Supplementary Information for details.

'Stim + non-optimally oriented flank'), had no effect on the signal. Neither did we see any suppression when moving the modulatory bar to a mirror-image position in visual space, at the same distance from the receptive field of the test neuron but far from the flank receptive field (Fig. 3, 'Far flank'). Note that the responses of the test and flank neurons were still significantly cross-correlated—implying a strong physiological connection between them—even when stimulating the flank resulted in a suppression of the test response (Fig. 3, lower left; also see Fig. 4, insets, and Supplementary Information). The common input that presumably underlies the cross-correlation is likely to provide excitatory input through direct synaptic connections on the target neurons, whereas inhibitory input would come through an inhibitory interneuron and hence would be delayed with respect to the excitation[35] (inset, Fig. 2; numerical simulation in Fig. 4a, inset). This would result in an excitatory increase in common firing probability preceding any inhibitory decrease, leading to a correlation of the common input-induced spikes in the test and flank neurons, even though the net signal decrease due to inhibition could be larger than any net excitatory increase (see Fig. 4, insets, and Supplementary Information for a quantitative model of this effect).

The suppression induced by a flanking perpendicular stimulus became stronger as the test recording site came closer to the cortical region activated by the flank stimulus. This is illustrated in Fig. 5a where we compare the suppression induced by a common flanking stimulus in two separate, simultaneously recorded test neurons with overlapping receptive fields but with recording sites at different cortical distances from the flanking orthogonal cortical column. Figure 5b shows a configuration complementary to that in Fig. 5a. Here we compare the suppression induced in the same neuron by two different flank stimuli equidistant from the test receptive field in visual space but corresponding to cortical columns at different anatomical distances from the recording site. Once again, the flanking stimulus that drove cells in the cortical column anatomically closer to the test site induced a significantly stronger suppression. By plotting the two-dimensional receptive field profile for the test neuron using an automated process (Fig. 5b; see Methods) we confirmed that the two flanking stimuli were symmetrically placed outside the classical receptive field of the neuron. This controls for the possibility that the stronger suppression caused by the 'near' flank could result from a trivial asymmetry in placement around the test receptive field, or to an asymmetry in the test receptive field profile leading to unequal engagement with the two flanks. In Fig. 5c we show that the pattern of flank suppression illustrated in Fig. 5a and b is mirrored over the entire population of near/far pairs recorded (31 pairs), whether with pairs of test sites that were near or far from a cortical flank column (Fig. 5a), or with flank cortical columns that were near or far from a common test site (Fig. 5b). For each pair in the population (with two exceptions: Fig. 5c) the near configuration produced a stronger suppression—by a factor of about 3 on average—than the corresponding far configuration.

We used a quantitative model of the overlap of a neuron's arborization with nearby cortical columns to show that the measured strength of flank suppression was proportional to the expected overlap with the corresponding cortical flank (Fig. 4). By using vascular landmarks, each test site was located on the corresponding optical image of the orientation map. The basin of local interactions feeding into the neuron was modelled as a circularly symmetrical gaussian centred on the recording site and extending roughly 800 μm (see Methods for details). Figure 4a shows the model for a particular recording site. The strength of interaction with a given orthogonal cortical column was modelled as the weighted overlap of the gaussian with the area covered by the cortical column in the optical map. Larger values for this overlap represented a combination of greater proximity of the given recording site to the cortical flank in question and a larger cortical area of orthogonal orientation in the flank. Figure 4b shows the pooled results for 60 test sites, with the experimentally measured strength of flank suppression plotted as a function of the modelled arborization overlap. The measured suppression is linearly proportional to the calculated overlap ($n = 60$ recording sites in 11 animals; regression $R^2 = 0.39$ when excluding the two pairs of points in which 'near' suppression is weaker than 'far' (Fig. 5c); $R^2 = 0.25$ when including these two pairs of points). This result indicates that even a simple geometric model of arborization overlap gives a plausible measure of the strength of local interactions that could underlie the suppression of neuronal activity by nearby perpendicular flanks.

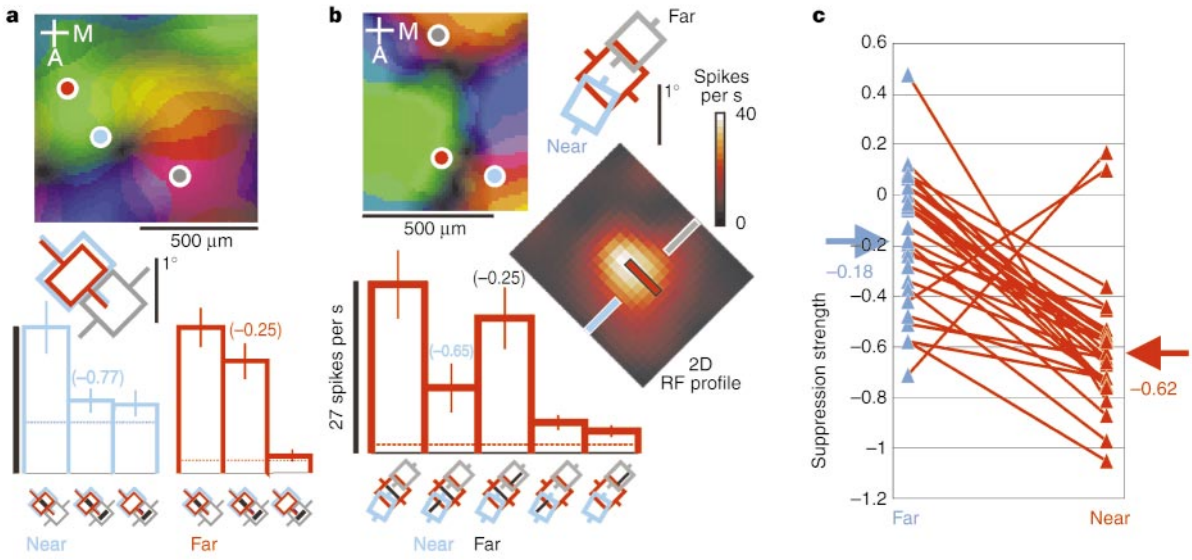

Figure 5 Flanks originating from nearer cortical loci lead to stronger suppression. **a**, Comparing simultaneously recorded test neurons, near (blue) and far (red) from the flank region (grey recording site and receptive field). The response histograms, stimulus configuration key and corresponding suppression are shown as in Fig. 3. **b**, Comparing the influence of a near (blue) and far (grey) flank, respectively. The test (red) and the two flank stimuli are shown overlaid, to scale, on the 2D profile of the test receptive field (see Methods). **c**, Comparing suppression strength for all far/near pairs (31 pairs, 12 cats; each pair connected by a line) quantified as in Fig. 3. Arrowheads show the mean value of suppression for each condition.

Discussion

Our results have a number of possible consequences for our understanding of both the general principles of cortical circuitry and local processing, and the particular mechanisms and architecture underlying the processing of complex visual stimuli.

Our first finding is that the strength of local cortical interactions is a graded function of cortical distance with a spatial scale matching the periodicity of cortical maps and independent of relative orientation. This provides a basis for a general principle that could underlie cortical processing. The effective local functional environment and local circuits affecting a neuron in V1 would depend critically on its location within the interrelated maps of position and orientation. The map of retinotopy over the surface of V1 is locally inhomogeneous, in register with inhomogeneities in the map of orientation[12]. In particular, neurons in cortical columns of mutually orthogonal orientation, lying on either side of an orientation singularity, represent non-overlapping (albeit abutting) regions of visual space. In cortical regions where orientation changes are relatively gradual, by contrast, the representation of space changes slowly. The current finding supports our proposal that neurons situated near orientation singularities could be engaged in local computations of visual features that are locally maximally dissimilar, through interactions with neighbouring orientation columns, and neurons in cortical regions of smoothly changing orientation could be engaged in computations of features that are maximally similar[12]. This could be a general motif in local cortical processing, resulting from the close match between the spatial scales of local interactions and the periodicity of the cortical map. Through local circuitry, an anatomically homogenous population of cortical neurons could thus achieve the widest possible dynamic range of any given response property by being distributed over a range of positions within—and having a corresponding range of overlaps with—a full set of cortical functional columns[36–38]. A functional 'module' on V1 would therefore comprise a cortical region containing a full range of such local neuronal circuits. These modules would have the same spacing over the cortical surface as the singularities in the map of orientation, with each module containing a full representation of all orientations covering a local region of visual space. These proposed modules would thus exhibit the same spacing, coverage and magnification as the 'ice cube' modular architecture proposed for V1 (ref. 38). Note that the cortical calculations proposed for these modules involve local neural circuitry that operates within the ambit of neighbouring cortical columns. This is to be distinguished from long-range horizontal connections over larger cortical distances that connect columns of similar orientation preference across different local modules. Visual interactions mediated by local connections are thus likely to operate at a smaller spatial scale than the processing that has been attributed to the long-range horizontal connections.

Our findings reveal a new set of response properties in V1 generated by local cortical interactions: a set of graded specializations for processing locally complex visual features. Increasing evidence indicates that cells in V1 are context dependent and that their responses may be specific for more complex stimulus configurations than a single oriented line segment[1]. The pattern of perpendicular flank modulation indicates that neurons might be functionally specialized for processing corners and T-junctions of particular handedness and relative layout. Different neurons in the same orientation column—which otherwise have similar orientation preferences and overlapping receptive fields—would show different degrees of this specialization; this could therefore be another response property with which to classify receptive fields, along with orientation, ocular dominance, disparity and so on. The purely suppressive modulation by perpendicular flanks seen here could signal the presence of corners or T-junctions by terminating the facilitatory modulation that propagates along cortical representations of smooth contours[2]. It could, alternatively, result from this study's being carried out in anesthetized animals, exposing a state of the cortical circuit unmodulated by attention or task demands[17,39–41]. Note that our findings deal with the role of local interactions in mediating the contextual influence that flanking lines exert on neuronal responses to simple stimuli. Local intracortical interactions have also been postulated to play a part in the shaping of the classical response properties of neurons. It has been suggested that the sharpness and dynamics of orientation or direction tuning of neurons in the upper layers of V1 could be determined by lateral intracortical connections operating over the same lateral scales as seen here[42]. Local inactivation in V1 leads to increases in the width of orientation tuning, or changes in direction selectivity, in an orientation-dependent manner supportive of a role for inhibition in maintaining such receptive field response properties in neurons in the upper layers of VI (refs 43, 44). The above studies deal with the forming of a neuronal response to a single line stimulus rather than the modulation of responses to a preferred stimulus through the presence of nearby flanking stimuli, and thus address an issue of distinctly different consequences for visual processing.

Like orientation preference, selectivity for more complex forms could have a systematic functional architecture. For neurons in the same orientation column, the degree of selectivity for processing corners is tied to the location of a neuron within the column, in a manner that can be predicted using a simple model of the overlap of the neuron's arborization with local features in the cortical map. This indicates that the parameter of corner processing could also form a functional map over the cortical surface, similar to and closely linked with the familiar maps of orientation and space. The evidence for this particular functional specialization raises the question of how diverse a group of distinct contextual interactions the primary visual cortex could encode. Even a generous estimate of the number of neurons required to represent a complete set of simple visual elements of orientation, disparity and ocular dominance in a local region of visual space leaves an apparent 100- to 1000-fold redundancy in the number of cortical neurons engaged in such a representation. This apparent redundancy is progressively reduced when we consider cortical responses to more complex stimuli; adjacent neurons, although displaying similar orientation preferences, have widely divergent responses to stimuli such as checker-board patterns[45]. The particular functional specialization reported here could prove to be just one of a much larger group of functional specializations mediated through local circuits and systematically organized over the surface of VI. □

Methods

Adult cats were anaesthetized, paralysed and prepared for electrical and optical recording from V1. Eyes were fixed relative to the stereotaxic apparatus by using a ring glued to the sclera.

Optical imaging. The orientation map on V1 was visualized by optically imaging the intrinsic cortical signal, as described[12]. The computed orientation vector at each point is colour coded for orientation preference at 11.25° intervals starting with blue (bin 0° to 11.25°; see key to left of optical image, Fig. 1a). The brightness of each colour indicates the strength of the computed orientation vector, with dark points or lines indicating singularities or fractures.

Electrophysiology. All electrical recordings were done using pairs of independently positioned electrodes (etched tungsten in varnish), to have a reference receptive field to monitor eye position. Receptive fields were single unit, isolated by setting the level of the spike discriminator at 3× to 5× the baseline and estimating by eye the constancy of the shape of the selected waveform (amplifier: AM Systems; spike discriminator: Tucker-Davis SD1), and were obtained within the first 300 μm—typically, within the first 150 μm—of the cortical surface. Receptive field boundaries were plotted by hand as minimum response fields.

2D receptive field profile. Response histogram obtained while a single test bar was flashed in pseudo-random sequence at the vertices of an $M \times N$ (typically 6×5) grid centred over the hand-plotted receptive field profile.

Peristimulus time histograms and orientation tuning curves. Oriented bar stimuli (size range: 0.25° × 0.1° to 1° × 0.25°; luminance range 7–15 cd m^{-2} against a background of 2.5 cd m^{-2}) were drifted at 1° s^{-1} and averaged over 5–15 sweeps. Orientation tuning curves were obtained by averaging over the corresponding peristimulus time histograms (PSTHs).

Cross-correlation. Calculated from spike trains of 2,000–10,000 spikes per neuron, 0.1 ms resolution, induced by drifting bars; using regions of PSTHs that were flat (within a factor of 2) for >1 s. Correlogram window, ± 100 ms, bin width 0.5 ms. Correlograms were corrected by the averaged shift predictor[31] (also known as shuffled correlogram or baseline): $X\text{-}Corr_{\mathrm{SHIFTED,AVG}} = \Sigma(X\text{-}Corr_{\mathrm{SHIFTED},I})/(N-1)$ (where $X\text{-}Corr_{\mathrm{SHIFTED},I}$ is the cross-correlogram obtained by shifting by an integral number I of sweeps), smoothed using a 5-bin kernel: [0.05, 0.25, 0.4, 0.25, 0.05] and normalized by the average baseline (over the correlogram window). The height and integrated area of the normalized cross-correlogram peak was used as our measure of the 'effective connection strength' linking the neuron pair under study[27,28,31]. Error estimates: for the peaks, standard deviation was equal to the standard deviation in the flanks of the normalized correlogram; for the area, the variance was estimated as the variance of the normalized correlogram, integrated over the width of the peak.

Population distribution of cross-correlation strength. The full population of 85 neuron pairs was divided into two groups: 'similar orientation pairs' (relative orientation difference <30°; 33 pairs) and 'orthogonal orientation pairs' (relative orientation difference >60°; 52 pairs).

Quantifying suppression by flank stimulus. ((Response to Stim + flank) − (Response to Stim alone))/(Response to Stim alone), after correcting for spontaneous activity.

Simulation of suppression by flank. Test and flank neurons, as well as 'common units' in test and flank cortical columns, were simulated as independent Poisson spike generators with variable rate. Spikes in either 'common' unit led to an excitatory increase followed by an inhibitory decrease in Poisson rate in both the test and flank neurons. The resultant spike trains were cross-correlated and normalized exactly like the real data. For details, see Supplementary Information.

Model of arborization overlap. The basin of common input interactions F(x, y) feeding from points (x, y) on cortex into a neuron at a given recording site (x_0, y_0) was equated to a normalized gaussian weighting function, $F(x,y) = A\exp(-(r/577)^2)$ with $r = \sqrt{((x-x_0)^2+(y-y_0)^2)}$ in μm and $A = 1/(\pi(577)^2)$. The spatial scale length of 577 μm was selected so that the amplitude of the gaussian fell to 0.15 times the peak at $r = 800$ μm. The relevant optical image was remapped in terms of orientation relative to the value at (x_0, y_0) and the orthogonal cortical columns were identified. The flank stimulus was assumed to drive cortical columns in an orientation-weighted manner: regions orthogonal ±15° at full strength, regions between 15° and 22.5° away from orthogonal at half strength and those between 22.5° and 30° away from orthogonal at one-quarter strength. The corresponding areas of the optical map were integrated and weighted by the orientaion-dependent weighting as well as by the gaussian arborization function, to give the final modelled value of arborization overlap with the flank cortical column.

Received 11 January; accepted 26 April 1999.

1. Gilbert, C. D. Adult cortical dynamics *Physiol. Rev.* **78,** 467–485 (1998).
2. Kapadia, M. K., Ito, M., Gilbert, C. D. & Westheimer, G. Improvement in visual sensitivity by changes in local context: parallel studies in human observers and in V1 of alert monkeys. *Neuron* **15,** 843–856 (1995).
3. Gilbert, C. D. Horizontal integration and cortical dynamics. *Neuron* **9,** 1–13 (1992).
4. Polat, U., Mizobe, K., Pettet, M. W., Kasamatsu, T. & Norcia, A. M. Collinear stimuli regulate visual responses depending on cell's contrast threshold. *Nature* **391,** 580–584 (1998).
5. Wertheimer, M. *Laws of Organization in Perceptual Forms* (Harcourt, Brace and Jovanovich, London, 1938).
6. Ullman, S. Three-dimensional object recognition. *Cold Spring Harbor Symp. Quant. Biol.* **55,** 889–898 (1990).
7. Field, D. J., Hayes, A. & Hess, R. F. Contour integration by the human visual systems: evidence for a local "association field". *Vision Res.* **33,** 173–193 (1993).
8. Hubel, D. H. & Wiesel, T. N. Sequence regularity and geometry of orientation columns in the monkey striate cortex. *J. Comp. Neurol.* **158,** 267–294 (1974).
9. Ts'o, D. Y., Frostig, R. D., Lieke, E. E. & Grinvald, A. Functional organization of primate visual cortex revealed by high resolution optical imaging. *Science* **249,** 417–420 (1990).
10. Blasdel, G. G. & Salama, G. Voltage-sensitive dyes reveal a modular organization in monkey striate cortex. *Nature* **321,** 579–585 (1986).
11. Bonhoeffer, T. & Grinvald, A. Iso-orientation domains in cat visual cortex are arranged in pinwheel-like patterns. *Nature* **353,** 429–431 (1991).
12. Das, A. & Gilbert, C. D. Distortions of visuotopic map match orientation singularities in primary visual cortex. *Nature* **387,** 594–598 (1997).
13. Malach, R., Amir, Y., Harel, M. & Grinvald, A. Relationship between intrinsic connections and functional architecture revealed by optical imaging and in vivo targeted biocytin injections in primate striate cortex. *Proc. Natl Acad. Sci. USA* **90,** 10469–10473 (1993).
14. Malach, R. Dendritic sampling across processing streams in monkey striate cortex. *J. Comp. Neurol.* **315,** 303–312 (1992).
15. Hubener, M. & Bolz, J. Relationships between dendritic morphology and cytochrome oxidase compartments in monkey striate cortex. *J. Comp. Neurol.* **324,** 67–80 (1992).
16. Katz, L. C., Gilbert, C. D. & Wiesel, T. N. Local circuits and ocular dominance columns in monkey striate cortex. *J. Neurosci.* **9,** 1389–1399 (1989).
17. Bosking, W. H., Zhang, Y., Schofield, B. & Fitzpatrick, D. Orientation selectivity and arrangement of horizontal connections in tree shrew striate cortex. *J. Neurosci.* **17,** 2112–2127 (1997).
18. Sillito, A. M., Grieve, K. L., Jones, H. L., Cuderio, J. & Davis, J. Visual cortical mechanisms detecting focal orientation discontinuities. *Nature* **378,** 492–496 (1995).
19. Shevelev, I. A., Novikova, R. V., Lazareva, N. A., Tikhomirov, A. S. & Sharaev, G. A. Sensitivity to cross-like figures in the cat striate neurons. *Neuroscience* **69,** 51–57 (1995).
20. Shevelev, I. A., Lazareva, N. A., Sharaev, G. A., Novikova, R. V. & Tikhomirov, A. S. Selective and invariant sensitivity to crosses and corners in cat striate cortex neurons. *Neuroscience* **84,** 713–721 (1998).
21. Gilbert, C. D. & Wiesel, T. N. Morphology and intracortical projections of functionally characterised neurones in the cat visual cortex. *Nature* **280,** 120–125 (1979).
22. Gilbert, C. D. & Wiesel, T. N. Clustered intrinsic connections in cat visual cortex. *J. Neurosci.* **3,** 1116–1133 (1983).
23. Ts'o, D. Y., Gilbert, C. D. & Wiesel, T. N. Relationships between horizontal corticocortical connections in cat visual cortex. *J. Neurosci.* **9,** 2432–2442 (1989).
24. Gilbert, C. D. & Wiesel, T. N. Columnar specificity of intrinsic horizontal and corticocortical connections in cat visual cortex. *J. Neurosci.* **9,** 2432–2442 (1989).
25. Grinvald, A., Lieke, E. E., Frostig, R. D., Gilbert, C. D. & Wiesel, T. N. Functional architecture of cortex revealed by optical imaging of intrinsic signals. *Nature* **324,** 361–364 (1986).
26. Frostig, R. D., Lieke, E. E., Ts'o, D. Y. & Grinvald, A. Cortical functional architecture and local coupling between neuronal activity and the microcirculation revealed by in vivo high resolution optical imaging of intrinsic signals. *Proc. Natl Acad. Sci. USA* 6082–6086 (1990).
27. Das, A. & Gilbert, C. D. Receptive field expansion in adult visual cortex is linked to dynamic changes in strength of cortical connections. *J. Neurophysiol.* **74,** 779–792 (1995).
28. Aertsen, A. M. H. J. & Gerstein, G. L. Evaluation of neuronal connectivity: sensitivity of cross-correlation. *Brain Res.* **340,** 341–354 (1985).
29. Perkel, D. H., Gerstein, G. L. & Moore, G. P. Neuronal spike trains and stochastic point processes. I The single spike train. *Biophys. J.* **7,** 391–418 (1967).
30. Perkel, D. H., Gerstein, G. L. & Moore, G. P. Neuronal spike trains and stochastic point processes. II Simultaneous spike trains. *Biophys. J.* **7,** 419–440 (1967).
31. Melssen, W. J. & Epping, W. J. M. Detection and estimation of neuronal connectivity based on crosscorrelation analysis. *Biol. Cybern.* **57,** 403–414 (1987).
32. Hata, Y., Tsumoto, T., Sato, H. & Tamura, H. Horizontal interactions between visual cortical neurones studied by cross-correlation analysis in the cat. *J. Physiol.* **441,** 593–614 (1991).
33. Kisvarday, Z. F. *et al.* Synaptic targets of HRP-filled layer III pyramidal cells in the cat striate cortex. *Exp. Brain Res.* **64,** 541–552 (1986).
34. McGuire, B. A., Gilbert, C. D., Rivlin, P. K. & Wiesel, T. N. Targets of horizontal connections in macaque primary visual cortex. *J. Comp. Neurol.* **305,** 370–392 (1991).
35. Hirsch, J. & Gilbert, C. D. Synaptic physiology of horizontal connections in the cat's visual cortex. *J. Neurosci.* **11,** 1800–1908 (1991).
36. Malach, R. Cortical columns as devices for maximizing neuronal diversity. *Trends Neurosci.* **17,** 101–104 (1994).
37. Bauer, U., Scholz, M., Levitt, J. B., Obermayer, K. & Lund, J. S. A model for the depth-dependence of receptive field size and contrast sensitivity of cells in layer 4C of macaque striate cortex. *Vision Res.* **39,** 613–629 (1999).
38. Hubel, D. H. & Wiesel, T. N. Functional architecture of macaque monkey visual cortex. *Proc. R. Soc. Lond. B* **198,** 1–59 (1977).
39. Ito, M. & Gilbert, C. D. Attention modulates contextual influences in the primary visual cortex of alert monkeys. *Neuron* **22,** 593–604 (1999).
40. Crist, R. E., Ito, M., Westheimer, G. & Gilbert, C. D. Task dependent contextual interactions in the primary visual cortex of primates trained in hyperacuity discrimination. *Abstr. Soc. Neurosci.* **23,** 1543 (1997).
41. Ito, M., Westheimer, G. & Gilbert, C. D. Attention and perceptual learning modulate contextual influences on visual perception. *Neuron* **20,** 1191–1197 (1998).
42. Sompolinsky, H. & Shapley, R. New perspectives on the mechanism for orientation selectivity. *Curr. Opin. Neurobiol.* **7,** 514–522 (1997).
43. Crook, J. M., Kisvárday, Z. F. & Eysel, U. T. GABA-induced inactivation of functionally characterized sites in cat striate cortex: effects on orientation tuning and direction selectivity. *Vis. Neurosci.* **14,** 141–158 (1997).
44. Crook, J. M., Kisvárday, Z. F. & Eysel, U. T. Evidence for a contribution of lateral inhibition to orientation tuning and direction selectivity in cat visual cortex: reversible inactivation of functionally characterized sites combined with neuroanatomical tracing techniques. *Eur. J. Neurosci.* **10,** 2056–2075 (1998).
45. Gawne, T. J., Kjaer, T. W., Hertz, J. A. & Richmond, B. J. Adjacent visual cortical complex cells share about 20% of their stimulus-related information. *Cerebral Cortex* **6,** 482–489 (1996).

Supplementary information is available on *Nature*'s World-Wide Web site (http://www.nature.com) or as paper copy from the London editorial office of *Nature*.

Acknowledgements. We thank A. Glatz and J. Lopez for expert technical assistance. The work was supported by the National Science Foundation.

Correspondence and requests for materials should be addressed to C.D.G. (e-mail: gilbert@rockvax.rockefeller.edu).